Disk-shaped Compact Tension Test for Asphalt Concrete Fracture

by M.P. Wagoner, W.G. Buttlar and G.H. Paulino

ABSTRACT—A disk-shaped compact tension (DC(T)) test has been developed as a practical method for obtaining the fracture energy of asphalt concrete. The main purpose of the development of this specimen geometry is the ability to test cylindrical cores obtained from in-place asphalt concrete pavements or gyratory-compacted specimens fabricated during the mixture design process. A suitable specimen geometry was developed using the ASTM E399 standard for compact tension testing of metals as a starting point. After finalizing the specimen geometry, a typical asphalt concrete surface mixture was tested at various temperatures and loading rates to evaluate the proposed DC(T) configuration. The variability of the fracture energy obtained from the DC(T) geometry was found to be comparable with the variability associated with other fracture tests for asphalt concrete. The ability of the test to detect changes in the fracture energy with the various testing conditions (temperature and loading rate) was the benchmark for determining the potential of using the DC(T) geometry. The test has the capability to capture the transition of asphalt concrete from a brittle material at low temperatures to a more ductile material at higher temperatures. Because testing was conducted on ungrooved specimens, special care was taken to quantify deviations of the crack path from the pure mode I crack path. An analysis of variance of test data revealed that the prototype DC(T) can detect statistical differences in fracture energy resulting for tests conducted across a useful range of test temperatures and loading rates. This specific analysis also indicated that fracture energy is not correlated to crack deviation angle. This paper also provides an overview of ongoing work integrating experimental results and observations with numerical analysis by means of a cohesive zone model tailored for asphalt concrete fracture behavior.

KEY WORDS—Asphalt concrete, fracture energy, disk-shaped compact tension, crack deviation, cohesive zone model

Introduction

Asphalt concrete is used as the surface layer on many types of pavements, due to its ease of construction, its ability to deliver a smooth and quiet riding surface, and its relatively low cost. However, various forms of fracture constitute a major source of premature deterioration for asphalt pavement

M.P. Wagoner is a Graduate Research Assistant, W.G. Buttlar is an Associate Professor, and G.H. Paulino (paulino@uiuc.edu) is an Associate Professor, Department of Civil and Environmental Engineering, University of Illinois at Urbana-Champaign, 205 North Mathews Avenue, Urbana, IL 61801, USA.

surfaces, particularly in colder climates.[1] The loading conditions that create cracks in asphalt concrete are thought to be a combination of mechanical (wheel loads) and environmental (thermal cycling and material aging) effects. In current design approaches, an empirical relationship is used to predict the fracture resistance of asphalt concrete from conventional engineering material parameters, such as modulus and tensile strength.[2] In order to significantly improve pavement design methods, the mechanisms behind the initiation and propagation of cracks in asphalt concrete must be better understood. The use of fracture mechanics and the development of valid fracture tests are arguably indispensable steps in the evolution of performance-based pavement design. Fracture mechanics has been used intermittently since the early 1970s[3] to analyze the fracture behavior of asphalt concrete. However, with recent advances in the mechanics field related to the fracture of quasi-brittle materials, the ability to accurately describe fracture mechanisms in asphalt concrete is now a plausible endeavor.[4,5]

Standardized fracture tests and fracture properties for asphalt concrete have not yet been developed to the extent that reliable measurements of fracture properties can be routinely determined. The single-edge notched beam (SE(B)) test has been the most common specimen geometry used in fracture testing of asphalt concrete.[3,6-9] The SE(B) geometry (Fig. 1(a)) has several qualities amenable to a reliable fracture test, such as simple loading configuration, large dimensions to reduce edge effects, and the stable propagation of mode I fracture. However, the SE(B) geometry has the disadvantage of requiring a non-standard specimen geometry, which limits its applicability to laboratory-compacted beams. It is often impractical to extract beam-shaped specimens from constructed pavement facilities. Cylindrical cores, on the other hand, are easily obtained with standard field coring equipment (Fig. 2). Figure 2 illustrates the condition of the field core when obtained from an area of high distress (such as a reflective crack). For the experimental use of the disk-shaped compact tension (DC(T)) test, the field cores would be obtained away from the distress, allowing for an intact specimen. The placement and direction of compaction of asphalt concrete can create an anisotropic material with a degree of preferential aggregate orientation towards the direction of compaction and variability in density along the thickness. The DC(T) test can only induce crack propagation oriented in the plane of the pavement for thin sections. Although some cracks may propagate in other directions (i.e., propagate upwards or downwards through the thickness), this appears to be an unavoidable circumstance when conducting DC(T) fracture tests on field specimens from pavements with thin layers. Thus, the
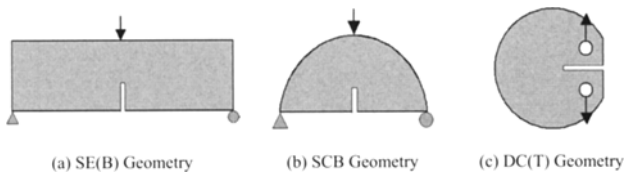
Fig. 1—Different fracture specimen geometries for asphalt concrete: (a) Single-edge notched beam;[3,6–9] (b) Semi-circular bend;[10,11] (c) Disk-shaped compact tension

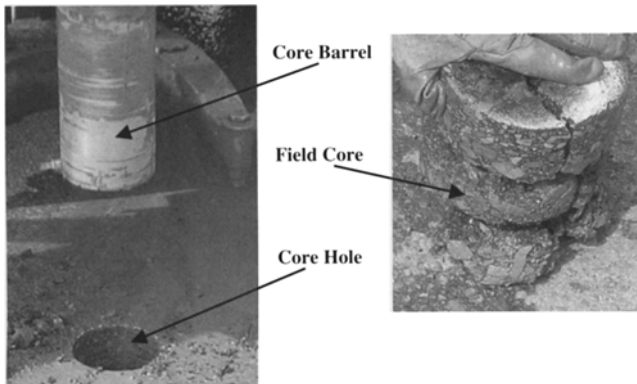| Recommended Dimensions (mm)	
D	150
W	110
ϕ	25
a	27.5
d	25
C	35

Fig. 2—Example of a core obtained at a reflective crack location in a pavement structure

Fig. 3—Recommended DC(T) geometry for asphalt concrete

current work is motivated by the need to characterize the fracture behavior of asphalt concrete from standard cylindrical field and laboratory specimens.

One prospective fracture test that can be performed using cylindrical samples is the semi-circular bend (SCB) test (Fig. 1(b)). The SCB test has been used to obtain the fracture toughness of asphalt concrete for use in estimating fatigue cracking[10] and for investigating the fracture energy of asphalt concrete at low temperatures.[11]

One concern with the SCB test arrangement for asphalt concrete is that the 150 mm diameter of a standard laboratory-compacted asphalt specimen leads to a relatively short fracture ligament in the SCB specimen. Without conclusive evidence of the size of the "fracture process zone"[4] of asphalt concrete (the relatively large grain size of the aggregates is apparent in Fig. 2), the initial ligament length should be as large as possible to produce a reliable fracture property and fracture test. Also, the crack propagation with the SCB geometry creates an arching effect with high compressive stress as the crack approaches the top edge. The high compressive stresses could arrest the crack, which further reduces the effective ligament, creating potentially invalid testing results.

Other geometries, such as notched direct tension,[12] have been used for obtaining fracture properties of asphalt concrete, but these geometries have the same limitation of being restricted to non-standard laboratory compaction procedures. Therefore, the development of a disk-shaped compact tension test (Fig. 1(c)) was pursued in this investigation.

Disk-shaped Compact Tension Geometry for Asphalt Concrete

The ASTM E399 Standard Test Method[13] describes the
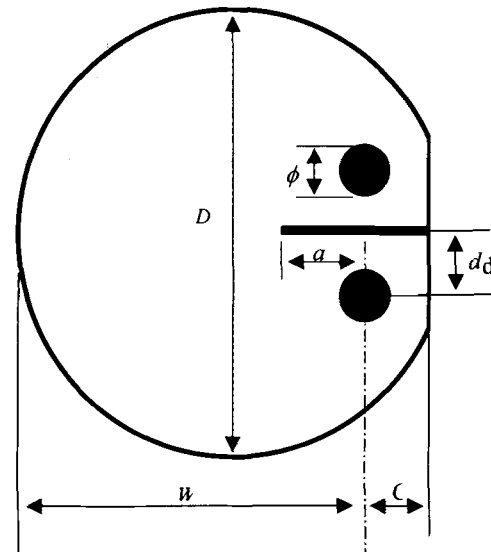
DC(T) specimen for obtaining the plane-strain fracture toughness of metallic specimens. A compact tension test has previously been used to obtain the fracture toughness of asphalt concrete;[14] however, the specimen geometry was of the standard rectangular-shaped form, which could not be easily fabricated from field cores or standard laboratory compaction methods.

The ASTM E399 specification was used as a starting point in this study for the development of a DC(T) specimen geometry for fracture testing of asphalt concrete. After several iterations in the laboratory, a specimen geometry that maximizes ligament length but prevents specimen rupture at the loading holes was developed. The resulting specimen dimensions are given in Table 1 along with the ASTM E399 dimensions. The proposed specimen geometry is schematically displayed in Fig. 3.

The dimensions of the proposed DC(T) specimen for asphalt concrete are within the tolerances given in the ASTM E399 specification, with the exception of the location of loading holes. During the developmental stages of the DC(T) geometry, the loading holes were placed closer to the edges of the specimen to create a longer ligament length. However, this geometry had a tendency to fail ($\sim$50% of the specimens) at the loading holes (see Fig. 4(a)) due to the geometrical configuration with insufficient material between holes and outer boundaries. The loading holes were moved towards the center of the specimen to ensure sufficient material was present and to reduce the chance of the specimen failing at the loading
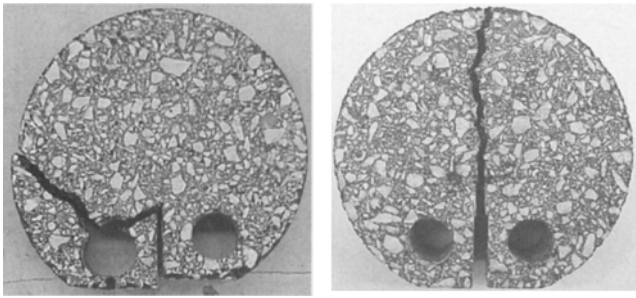
Fig. 4—Crack growth in the initial and final specimen geometry (a) initial specimen geometry with failure at the loading points; (b) final specimen geometry with desirable fracture plane

TABLE 1—COMPARISON OF DC(T) SPECIMEN DIMENSIONS GIVEN IN ASTM E399 AND THOSE RECOMMENDED FOR ASPHALT CONCRETE

	Dimensions in mm	
	ASTM E399	Recommended for Asphalt Concrete*
D	150	150
W	111	110
B_{max}	56	50
B_{min}	28	
C	28	35
ϕ	28	25
d	31	25
a_{max}	61	27.5
a_{min}	50	

* Based upon experiments on asphalt mixtures with 9.5 mm nominal maximum aggregate size and smaller

holes. After modifying the loading hole locations (Fig. 4(b)), over 80 specimens have been tested without a single failure at a loading hole.

Because the DC(T) geometry is being developed as a practical engineering fracture test, the specimen thickness (B) should reflect the typical pavement layer thicknesses present in the field (25–100 mm). For test repeatability, it is often recommended that the smallest dimension of the specimen be at least four times greater than the maximum aggregate size.[15] For this study, the maximum aggregate size in the mixture was 9.5 mm. A specimen thickness of 50 mm was selected for this study based upon these considerations. The influence of specimen thickness on fracture energy has been observed in Portland cement concrete[16] and deserves consideration for asphalt concrete. However, the investigation of such an effect was beyond the scope of this preliminary investigation.

The a/W ratio (see Fig. 3) for the present study was held constant at 0.25, which is less than the ASTM range of 0.45–0.55. The ASTM specification has this recommendation to ensure that the specimen meets the small-scale yielding criteria. The 0.25 a/W ratio was selected to provide a larger fractured face area, which should reduce the variability of the test results caused by heterogeneity of asphalt concrete.

In order for the DC(T) geometry to be practical, the fabrication of the specimen should also be straightforward. The specimen can be cut from a cylinder to the desired thickness

using a water-cooled masonry saw. Next, a template can be used to mark the location of the loading holes, the flat edge at the notch mouth, and the notch length. The specimen can then be mounted on an $X - Y$ table connected to a water-cooled core drill with a 25 mm outside diameter core barrel to core the loading holes. The use of a core drill was selected over other methods because the core barrel produces a smooth loading hole that is perpendicular to the specimen face. The $X - Y$ table was used to precisely locate the loading holes, reducing the chance of eccentricity during loading. The flat edge can be cut into the specimen using a water-cooled masonry saw. Careful consideration was taken in the fabrication of the mechanical notch. The ASTM specification has the requirement of a fatigue crack grown from the mechanical notch tip to produce a sharp crack tip. The ability to produce a fatigue crack of known length in asphalt concrete without damaging the surrounding material is questionable and may not be necessary if the width of the mechanical notch is narrow compared to the aggregate structure.[9] To efficiently achieve a narrow notch width, the mechanical notch was cut to approximately half of the intended length using a water-cooled masonry saw with a notch width of 5 mm. Then, the mechanical notch was finished using a handsaw with a carbide-grit blade, producing a notch width of approximately 1 mm. The two-step procedure was used to expedite the fabrication of the notch and the entire notch could be fabricated using the 1 mm wide saw blade as well.

Experimental Procedure

An experimental design was developed to determine the potential of using the DC(T) geometry for obtaining the fracture energy of asphalt concrete. A single mixture was used, consisting of a 9.5 mm maximum aggregate size with a PG64-22 asphalt binder. The PG64-22 asphalt binder, determined by the American Association of State Highway and Transportation Officials (AASHTO) MP1 Standard,[17] is a widely used asphalt binder for the climate found in central Illinois. The 9.5 mm maximum aggregate size mixture is typical of a surface layer in an asphalt concrete pavement. Cylindrical specimens were prepared in the laboratory following standard procedures using a gyratory compactor.[18] All specimens were compacted to 93±1% of the theoretical maximum density of the mixture. From each gyratory-compacted cylinder (115 mm high), two DC(T) specimens were fabricated with a 50 mm thickness following the procedures described above.

All testing was performed with an Instron 8500 servo-hydraulic load frame with an environmental chamber capable of controlling the temperature from 30°C to –30°C within ±0.1°C. The loading fixture was fabricated following the ASTM specification to ensure that the loading pins remained frictionless throughout the loading. Load was measured with a 10 kN load cell and the crack mouth opening displacement (CMOD) with an Epsilon Model 3541-0020-250-ST clip-on gage. Figure 5 shows the experimental setup with the loading fixtures, specimen, clip-on gage, and crack detection wires: one on the front (shown) and one on the back. The clip-on gage was used as the feedback for the control loop to ensure stable post-peak crack growth. The experimental design was developed to detect the changes of fracture energy at various temperatures (–20°C, –10°C, and 0°C) and loading rates (10, 5, 1, and 0.1 mm min^{-1}). At each temperature and rate, three replicates were tested to obtain the average fracture energy.
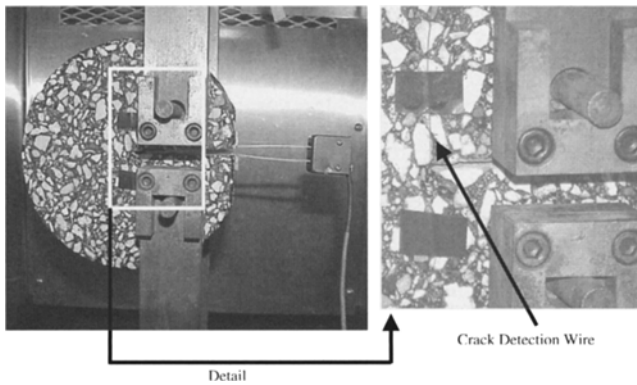
Fig. 5—Experimental setup for the DC(T) specimen with crack detection wire

Fig. 6—Load–CMOD curve for three experimental results ($a/W = 0.25$) at $-10°C$

Several proposed techniques were found in the literature for determining the fracture energy but, for this study, the fracture energy was computed as the area under the load–CMOD curve normalized by the area of the fractured surface (initial ligament length times specimen thickness). In the computation of fracture energy, unavoidable electronic noise in the sensors creates unreliable estimates of area under the load–CMOD curve. To circumvent this problem, the CMOD data were smoothed using linear regression through the CMOD–time curve. The use of linear regression is valid since the test was in fact controlled at a constant CMOD rate.

Test Results

For the DC(T) geometry to provide a useful fracture property, the variability of the fracture energy should be within an acceptable range. The repeatability of the test and the measured quantities (load and CMOD) influence the fracture energy, and understanding these curves provides insight into the fracture process. Figure 6 shows the load–CMOD curves for three replicates tested at $-10°C$ and 1 mm min^{-1} CMOD rate. For the three replicates, the initial stiffness and peak loads are very similar. The softening or post-peak responses of the replicates vary in shape and length of the softening tail. Crack detection wires have been placed at the notch tip (Fig. 5) to indicate when the macrocrack initiates, which typically occurs after peak load (see Fig. 6). However, it must be acknowledged that microcracking and localized damage occur throughout the loading, especially at peak load. The aggregate structure could have an effect on the crack path and thus the softening response. The crack path can traverse through aggregates, between aggregate–asphalt binder interfaces, or through the asphalt binder. The fracture energy associated with each of these paths is expected to be quite different. Since the aggregate structure for each test replicate is different, the softening response will likewise differ for the aforementioned reasons. The load–CMOD curves of Fig. 6 suggest that while the aggregate structure does not significantly affect the load required for crack initiation, it does lead to some scatter between replicates in the load–CMOD response after peak load is reached.

The coefficients of variation (COVs) of the fracture energy at each temperature and loading rate were obtained for compar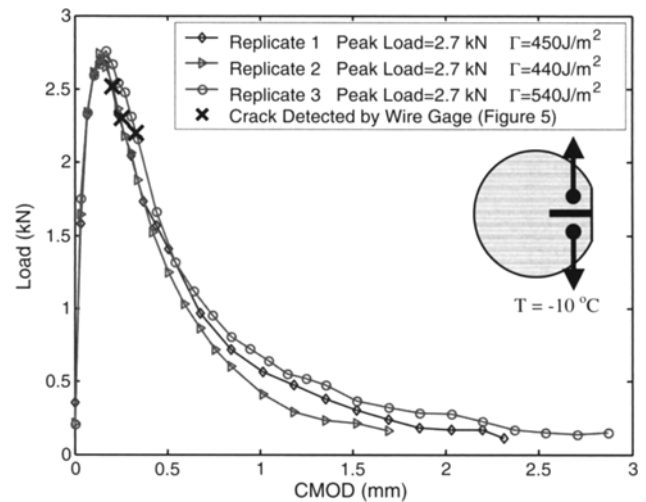ison (Table 2). In general, the COV decreases as the temperature increases. The reason for the increase in variability with decreasing temperature could be that the material is more brittle at lower temperatures, where defects (voids, weak aggregates, etc.) significantly influence the fracture process. Based upon visual observation of the fracture surface, the crack appeared to travel around aggregates at the highest temperature (0°C), whereas at the lowest temperature, the crack front often traveled through aggregates. Asphalt binder properties have a strong dependence on temperature, where the modulus and strength generally increase as the temperature decreases with the exception of binder strength at very low temperatures.[19] The COV from the DC(T) geometry was compared to the data found in the literature for the SE(B)[7] and SCB[11] geometries. The COV determined for the DC(T) geometry was within the range determined with the SE(B) (3–28%) and SCB (15–34%).

With satisfactory repeatability of fracture energy measurements, the next step was to assess the ability of the DC(T) test to detect the effects of temperature and loading rate on fracture energy. Asphalt concrete shows a transition from brittle to ductile fracture behavior as temperature increases. Figure 7 shows the load–CMOD curves for a single loading rate (1 mm min^{-1}) at the three test temperatures. The initial stiffness of the material decreases with increasing temperature (see Table 3) along with a change in the post-peak softening response. The curvature of the softening curve decreases as the temperature increases, suggesting more load carrying capacity, and thus more total energy is required to create the fracture surface. In this case, more energy is spent on inelastic deformation. The same phenomenon is seen for the loading rates where the material appears more brittle as loading rate increases. Table 2 shows the average fracture energy of three replicates at all temperatures and loading rates. In general, the fracture energy increases as the temperature increases, and energy decreases with increasing loading rate. The current analysis assumes the distribution of energy is dominated by fracture energy, but creep strain dissipation, distributed material damage, etc., will also consume energy. It is hoped that current work to couple the experimental observations with numerical analysis will lead to a truly fundamental material

TABLE 2—AVERAGE FRACTURE ENERGY AND COV OF THE FRACTURE ENERGY AT VARIOUS TEMPERATURES AND LOADING RATES (BASED UPON THREE REPLICATES)

Rate (mm min^{-1})	Fracture Energy (J m^{-2}) Temperature (°C)			COV (%) Temperature (°C)		
	−20	−10	0	−20	−10	0
10	41	276	407	14.5	8.7	13.0
5	197	318	397	25.4	12.3	10.3
1	233	328	470	17.4	14.0	4.2
0.1	245	352	848	15.9	14.5	8.8
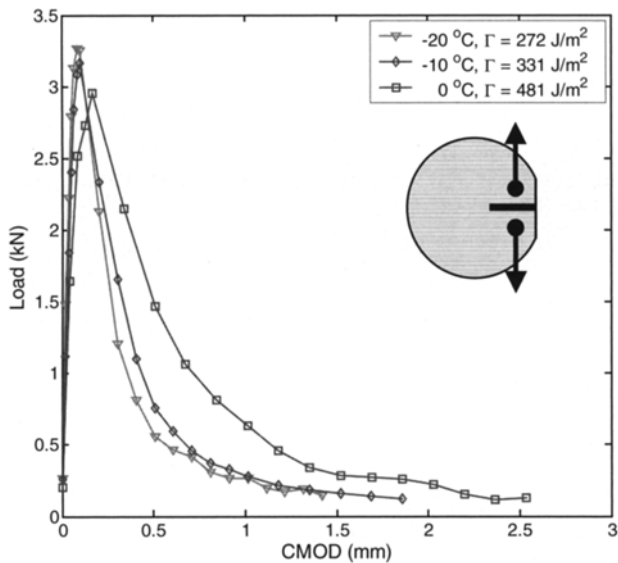
Fig. 7—Load–CMOD curves for 1 mm/min loading rate at three test temperatures

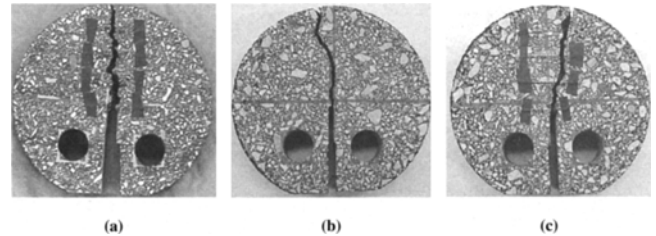Fig. 8—Three types of crack paths observed from the tests with the DC(T) geometry: (a) type I crack path; (b) type II crack path; (c) type III crack path

TABLE 3—INITIAL STIFFNESS FOR VARIOUS TEMPERATURES AT 1 mm/min LOADING RATE

Temperature (°C)	Initial Stiffness (kN mm^{-1})
−20	60.4
−10	45.9
0	32.4

property to be extracted from the DC(T) test. Concurrent testing of similar materials with the SE(B) test will be used to validate the analysis techniques, which are currently under development.

Discussion of Crack Trajectory

Although the test repeatability and the trends in the fracture energy were satisfactory, the observed deviations from the mode I crack path were a cause for concern. Three distinct types of crack paths were observed during the testing, as shown in Fig. 8. The mode I or straight crack path (termed type I) was the second most common crack path and was also the desired crack path. The most common crack path was the type II path, where the crack initiates in a straight path and then deviates at a point along the ligament. The final crack path, and also the least common, was the crack that initiates

and propagates at an angle from the notch tip. For elimination of crack deviation, side grooves could be fabricated in the specimen, but this would require extra steps in the fabrication procedure, which would be cumbersome and perhaps impractical. Table 4 shows the average crack deviation angles for three replicates at the temperatures and rates tested during this study. There are several possible causes for crack turning and crack deviation, such as the presence of larger and/or stronger aggregates in the crack path. Other possible factors include material heterogeneity and load eccentricity.

Statistical Analysis of Variance of Test Results

To support the observations that the fracture energy can detect changes with temperature and loading rate, an analysis of variance (ANOVA) was performed on the test data using SAS Version 9.1 software. Two separate hypotheses were tested: (1) statistically different values of fracture energy can be obtained with the proposed DC(T) test for the temperatures and loading rates selected for this study; (2) fracture energy is not correlated with crack deviation angle. To test the hypotheses, the p-value, or the smallest significance level at which the observed data would have caused rejection,[20] was used and set at 0.05. For the first hypothesis, the p-value is much less than the probability set (0.05) as shown in Table 5, indicating that statistically significant differences in fracture energy can be detected by the DC(T) tests among the test temperatures and loading rates studied. The second hypothesis that the crack deviation does not affect the fracture energy is also found to be true, as summarized in Table 6. The correlation between fracture energy and crack deviation is very low ($R = -0.048$) and the differences between the means do not differ significantly from zero (p-value = 0.7455).

Cohesive Zone Fracture Simulation of DC(T) Test

To gain insight into the fracture behavior of asphalt concrete, an integrated approach is being undertaken by coupling

TABLE 4

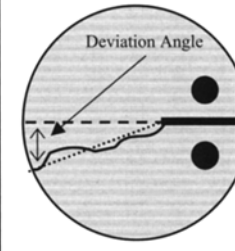| Rate (mm/min)	Temperature (°C)			Average
	0	-10	-20	
10	7	4	8	6
5	6	7	8	6
1	3	7	3	5
0.1	7	4	3	4
Average	6	5	5	
Overall Average	5			

TABLE 5—ANOVA TABLE FOR COMPARING FRACTURE ENERGY TO TEMPERATURE AND LOADING RATE

Source	DF	Type III SS	Mean Square	F-value	$Pr > F$
Temperature	2	751612.06	375806.03	216.78	<0.0001
Loading	3	280113.89	93371.30	53.86	<0.0001
Temperature *Loading	6	222008.61	37001.44	21.34	<0.0001

TABLE 6—CORRELATION TABLE BETWEEN CRACK DEVIATION AND FRACTURE ENERGY

Pearson Correlation Coefficients (R), $N = 48$		
	Deviation	Energy
Deviation	1.00000	-0.04809 (0.7455)[a]
Energy	-0.04809 (0.7455)[a]	1.00000

[a]The p-value where prob > $|r|$ under H_0: Rho = 0.

Fig. 9—Comparison of experimental data with numerical analysis using a bilinear cohesive zone model

experimental results and observations with numerical analysis. Thus, the experimental results of the DC(T) can be used to calibrate a conventional fracture mechanics model, as illustrated by Fig. 9. The current numerical approach consists of a non-linear finite element method (FEM) with an intrinsic cohesive zone model (CZM) to capture fracture behavior.[21,22] For preliminary computational analysis of the DC(T), a two-dimensional FEM discretization is considered with linearly elastic elements to model the bulk material behavior and interface cohesive elements to model the crack.[21] Although asphalt concrete is a viscoelastic material,[1] linear elasticity can be satisfactorily applied to model laboratory results with the proper selection of the complex (dynamic) modulus. In this case, an elastic modulus of $E = 14.2$ GPa (1 Hz loading at $-10°C$) and Poisson's ratio $\nu = 0.35$ were used. The intrinsic CZM adopted here is a bilinear-type model,[23] which requires two independent separation-material properties as input: tensile strength (σ_t) and fracture energy (G_f). Moreover, the initial slope of the model can be adjusted to reduce undesirable compliance effects.[23,24] The tensile strength $(\sigma_t = 3.56$ MPa) was determined using the Superpave Indirect Tensile Test Device.[25] The fracture energy obtained from the DC(T) test at $-10°C$ and 1 mm min^{-1} loading rate was used.

The numerical analysis fits the load–CMOD response of the DC(T) test well and leads to the calibrated results of Fig. 9 obtained with 1.0 G_f and 0.74 σ_t. Very recently, this modeling has successfully been extended to include a viscoelastic description of the bulk material,[24] i.e., the volumetric mat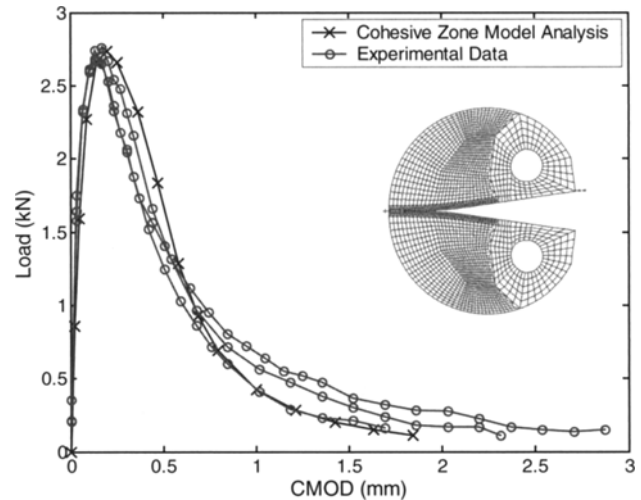erial (as opposed to the "separation material" that has its fracture behavior described by means of a cohesive zone model). Using a calibrated viscoelastic model, additional insights have been gained towards the advantages of the DC(T) testing mode, including the following.

1. The integration of the model and experiment allows the analyst to isolate the energy required to create the fracture surfaces from other sources of energy dissipation, including viscous effects.

2. For viscoelastic materials such as asphalt concrete, the compact tension test has a significantly lower portion of the measured energy that can be attributed to viscous effects as compared to SE(B) testing.

Cohesive zone modeling of fracture behavior in asphalt concrete appears to be very promising, and additional work that integrates modeling, laboratory experiments, and field behavior is presently under investigation by the authors.

Summary and Conclusions

In this paper we describe the development of a practical test to obtain the fracture energy of asphalt concrete from laboratory and field specimens. The DC(T) geometry is considered a practical specimen geometry that can be easily fabricated from cylindrical cores obtained from in-place pavements and from gyratory-compacted cylinders fabricated during the asphalt concrete design process. The dimensions of the DC(T) geometry for asphalt concrete were developed using the ASTM E399 specification as a guideline. Modifications were made to the loading hole locations to ensure that sufficient material was present to prevent localized failure at the loading points. Once the prototype test device was sufficiently developed, an experimental design was developed and carried out using a typical asphalt surfacing mixture. This mixture was tested over a full-factorial combination of three test temperatures and four loading rates with three test replicates for each combination.

Based upon the results of this investigation, the following conclusions can be drawn.

- The COV of the fracture energy obtained from the DC(T) geometry is comparable with the COV obtained in the literature for the SE(B) and SCB geometries, and is within an acceptable range.

- The fracture energy of asphalt concrete increases with increasing temperature, suggesting that the material undergoes a transition from brittle to ductile material. For the range of temperatures investigated ($-20°C$, $-10°C$, and $0°C$), the fracture energy increases as the loading rate decreases (see Table 2). This is a general observation, which is not specific to the DC(T) test presented here.

- The crack path for the ungrooved specimens tested in this study was found to deviate an average of 5° from the mode I crack trajectory. However, a statistical analysis of variance demonstrated that there was no correlation between fracture energy and angle of deviation for the data examined.

Thus, the DC(T) geometry appears to be a promising test for obtaining the fracture energy of asphalt concrete using a specimen geometry that is amenable for both laboratory and field-cored specimens. Further work needs to be conducted to fully understand the fracture energy that is obtained from the DC(T) geometry, including the following.

- Specimen size effect[22,26] has a significant impact on the fracture energy obtained from Portland cement concrete materials, and the size effect should be studied for asphalt concrete since the two materials both exhibit quasi-brittle fracture behavior. The thickness of the specimen influences the fracture energy[16] and an understanding of this three-dimensional effect should be developed since the thickness of in-place pavements vary, and thus the associated specimen thickness will vary.

- A preliminary investigation of the effect of crack deviation on the measured fracture energy has been conducted in the present work. However, this important effect deserves to be investigated in more detail (e.g.,

by means of multiscale analysis with explicit modeling of the local microstructure) to ensure that the obtained fracture energy is valid when the experimental crack trajectory deviates from the theoretical mode I path.

- The experimental determination of fracture energy appears to be satisfactory for asphalt concrete at low temperatures when the material is relatively stiff, but the determination of fracture energy at higher temperatures needs to be further investigated, since the material appears to have a large area of distributed damage ahead of the crack. Therefore, guidelines need to be developed to determine when the experimental results can be used to obtain valid fracture parameters.

To achieve these goals, additional work that integrates experimental results with numerical analysis will be pursued.

References

1. *Superpave Mix Design, Asphalt Institute Superpave Series No. 2 (SP2), 3rd edition (2001).*

2. Huang, Y.H., *Pavement Analysis and Design, Prentice-Hall, Englewood Cliffs, NJ (1993).*

3. Majidzadeh, K., Kauffmann, E.M., and Ramsamooj, D.V., "Application of Fracture Mechanics in the Analysis of Pavement Fatigue," *Journal of the Association of Asphalt Paving Technologists,* **40**, 227–246 (1971).

4. Anderson, T.L., *Fracture Mechanics: Fundamentals and Applications,* CRC Press, Boca Raton, FL (1995).

5. Kanninen, M.F. and Popelar, C.H., *Advanced Fracture Mechanics,* Oxford University Press, New York (1985).

6. Marasteanu, M.O., Labuz, J.F., Dai, S., and Li, X., "Determining the Low-temperature Fracture Toughness of Asphalt Mixtures," *Transportation Research Record* **1789**, 191–199 (2002).

7. Mobasher, B.M., Mamlouk, M.S., and Lin, H-M., "Evaluation of Crack Propagation Properties of Asphalt Mixtures," *ASCE Journal of Transportation Engineering,* **123** (5), 405–413 (1997).

8. Bhurke, A.S., Shin, E.E., and Drzal, L.T., "Fracture Morphology and Fracture Toughness Measurement of Polymer-modified Asphalt Concrete," *Transportation Research Record* **1590**, 23–33 (1997).

9. Wagoner, M.P., Buttlar, W.G., and Paulino, G.H., "Development of a Single-edge Notched Beam Test for Asphalt Concrete Mixtures," *ASTM Journal of Testing and Evaluation, in press.*

10. Hofman, R., Oosterbaan, S.M., Erkens, J.G., and van der Kooij, J., "Semi-circular Bending Test to Assess the Resistance Against Crack Growth," *Proceedings of the 6th RILEM Symposium on Performance Testing and Evaluation of Bituminous Materials, Zurich, Switzerland, 257–263 (2003).*

11. Li, X. and Marasteanu, M., "Evaluation of the Low Temperature Fracture Resistance of Asphalt Mixtures using the Semi-circular Bend Test," *Journal of the Association of Asphalt Paving Technologists,* **73**, 401–426 (2004).

12. Jacobs, M.M.J., Hopman, P.C., and Molenaar, A.A.A., "Application of Fracture Mechanics Principles to Analyze Cracking in Asphalt Concrete," *Journal of the Association of Asphalt Paving Technologists,* **65**, 1–39 (1996).

13. *ASTM E399-90, "Standard Test Method for Plane-strain Fracture Toughness of Metallic Materials," Annual Book of ASTM Standards, Vol. 03.01, ASTM International, 443–473 (2002).*

14. Collop, A.C., Sewell, A.J., and Thom, N.H., "Laboratory Assessment of the Resistance to Crack Propagation in High Stiffness Asphaltic

Materials," *IMechE Journal of Materials: Design and Applications*, **218**(*1*), 55–68 (2004).

15. Chehab, G.R., O'Quinn, E., and Kim, Y.R., "Specimen Geometry Study for Direct Tension Test Based on Mechanical Tests and Air Void Variation in Asphalt Concrete Specimen Compacted by Superpave Gyratory Compactor," *Transportation Research Record* **1723**, 125–132 (2000).

16. Duan, K., Hu, X-Z., and Wittmann, F.H., "Thickness Effect on Fracture Energy of Cementitious Materials," *Cement and Concrete Research*, **33**, 499–507 (2003).

17. AASHTO MP1-93, "Standard Specification for Performance Graded Asphalt Binder," *AASHTO Provisional Standards*, 1–4 (1996).

18. AASHTO TP4-00 "Method for Preparing and Determining the Density of Hot-mix (HMA) Specimen by Means of the Superpave Gyratory Compactor," *AASHTO Provisional Standards*, 290–294 (2000).

19. Olard, F., Di Benedetto, H., Eckmann, B., and Vaniscote, J., "Low-temperature Failure Behavior of Bituminous Binders and Mixes," *Proceedings of the 83rd Annual Meeting of the Transportation Research Board, Washington, DC (2004)*.

20. Miller, R.B. and Wichern, D.W., *Intermediate Business Statistics: Analysis of Variance, Regression, and Time Series, Dryden Press, Hinsdale, IL (1977)*.

21. Paulino, G.H., Song, S.H., and Buttlar, W.G., "Cohesive Zone Modeling of Fracture in Asphalt Concrete," *Proceedings of the 5th RILEM International Conference on Cracking in Pavements, May 5–7, Limoges, France (2004)*.

22. Bazant, Z.P. and Cedolin, L., *Stability of Structures: Elastic, Inelastic, Fracture, and Damage Theories, Oxford University Press, New York (1991)*.

23. Zhang, Z. and Paulino, G.H., "Cohesive Zone Modeling of Dynamic Failure in Homogeneous and Functionally Graded Materials," *International Journal of Plasticity*, **21**(*6*), 1195–1254 (2005).

24. Song, S.H., Paulino, G.H., and Buttlar, W.G., "Simulation of Crack Propagation in Aspalt Concrete Using a Cohesive Zone Model," *ASCE Journal of Engineering Mechanics*, submitted.

25. AASHTO TP9-96, "Standard Test Method for Determining the Creep Compliance and Strength of Hot Mix Asphalt (HMA) Using the Indirect Tensile Test Device," *AASHTO Provisional Standards*, 169–179 (1991).

26. Bazant, Z.P. and Planas, J., *Fracture and Size Effect in Concrete and Other Quasi-brittle Materials, CRC Press, Boca Raton, FL (1998)*.